Endocrine, *vol. 13, no. 1, 63–70, August 2000* 0969–711X/00/13:63–70/$12.00

Functional Interactions Between the Extracellular Domain and the Seven-Transmembrane Domain in Ca^{2+} Receptor Activation

Omar M. Hauache,[1] Jianxin Hu, Kausik Ray, and Allen M. Spiegel

Metabolic Diseases Branch, NIDDK, NIH, Bethesda, MD

We studied the activity of mutants involving the amino-terminal extracellular, seven-transmembrane (7TM) and carboxy-terminal tail domains of the human Ca^{2+} receptor to gain insight into the functional interactions between these domains during receptor activation. Missense mutations of highly conserved residues, D190 and E297, in the extracellular domain (ECD), and a mutation within part of the proximal carboxy-terminal tail, A877-880E, resulted in receptors with severely reduced response to Ca^{2+} despite adequate cell surface expression. Coexpression of either D190A or E297K mutants with A877-880E led to significant reconstitution of function. No such reconstitution occurred when D190A or E297K mutants were coexpressed with a truncation mutant possessing an intact amino-terminal extracellular and first transmembrane domain, despite evidence for heterodimerization and cell surface expression of the respective mutant receptors. In addition, no reconstitution of function was observed when D190A was coexpressed with a deletion Ca^{2+} receptor mutant lacking only a cysteine-rich region located in the ECD of the Ca^{2+} receptor (Ca-//-Ca). Moreover, coexpression of this Ca-//-Ca with A877-880E did not recover function. The results show that Ca2+ receptor extracellular and 7TM domains are discrete entities that can communicate within the context of a heterodimer composed of complementary mutant receptors. Two intact 7TM domains and two intact cysteine-rich regions appear to be required for such communication to occur. The results are discussed in the context of a speculative model of receptor structure and function.

Key Words: Calcium receptor; activation; functional interations.

Received April 12, 2000; Revised May 16, 2000; Accepted May 16, 2000.
Author to whom all correspondence and reprint requests should be addressed: Dr. Allen M. Spiegel, NIH, Bldg. 31, Rm 9A-52, Bethesda, MD 20892. E-mail: spiegela@extra.niddk.nih.gov
[1]O. M. Hauache was supported by a grant (#10848-2) from FAPESP (Fundacao de Amparo a Pesquisa do Estado de Sao Paulo, Brazil).

Introduction

The Ca^{2+} receptor (CaR) *(1)*, by influencing the rate of parathyroid hormone secretion from parathyroid cells and the rate of calcium reabsorption by the kidney, is involved in the control of extracellular Ca^{2+} ($[Ca^{2+}]_0$) homeostasis *(2)*. A number of naturally occurring loss-of-function mutations of the CaR have been identified in the autosomal dominantly inherited disease, familial hypocalciuric hypercalcemia (FHH), providing evidence for the importance of the CaR in normal regulation of $[Ca^{2+}]_0$ homeostasis *(2)*.

The CaR is a member of family 3 of the superfamily of G protein–coupled receptors (GPCRs) *(3)*, and is characterized, in addition to the seven-transmembrane (7TM) domain common to all GPCRs, by a large (approx 600 residue) amino-terminal extracellular domain (ECD) and a long (approx 200 residue) cytoplasmic carboxy-terminal tail (C-tail). The ECD and 7TM/C-tail of the CaR appear to be functionally separable domains based on studies with chimeric receptors *(4,5)*. The CaR ECD is thought to be the site of Ca^{2+} binding *(1,4,5)*, and by analogy with the metabotropic glutamate receptor (mGluR) ECD *(6)*, has been suggested to have a bilobed, venus-flytrap-like structure similar to that of bacterial periplasmic binding proteins (PBP) *(7,8)*. The 7TM/C-tail is presumed to be responsible for G protein coupling and activation *(9,10)*. A speculative model for CaR activation based on available data would suggest that Ca^{2+} binding to the ECD leads to a conformational change (closing of the venus flytrap) resulting in an interaction between the ECD and 7TM domains that leads to receptor activation.

Recent studies have demonstrated that the CaR is expressed at the cell surface as an intermolecular disulfide-linked dimer *(11,12)*, and that cotransfection of two inactive, mutant CaRs can lead to partial reconstitution of function, when the mutations involve separate domains (e.g., ECD and C-tail) of the CaR *(13)*. In order to probe further the functional interactions between the ECD and 7TM/C-tail of the CaR, we tested the ability of various mutant forms of the receptor to heterodimerize and reconstitute activity.

Results

Cell Surface Expresssion of Wild Type (WT) and Mutant CaRs

We studied five mutant forms of the CaR. Two are missense mutants, E297K and D190A, involving amino acids in the ECD. E297K is a naturally occurring mutation identified in FHH and shown to cause almost complete loss of Ca^{2+} response *(13)*. The D190A mutant was made to test the effect of mutating this aspartate residue, which is conserved in almost all GPCR family 3 members, including taste, mGluR, and some of the vomeronasal, putative pheromone receptors *(3,14)*. The A877-880E mutant changes three alanines in a portion of the C-tail previously shown to be critical for G protein activation *(10)*. We also studied TM1, a truncation mutant with an intact ECD and first transmembrane domain and a stop codon in the first intracellular loop *(8)*, and Ca-//-Ca, a cysteine-rich region deletion mutant *(15)*. Figure 1 depicts schematically the structure of the CaR and the location of mutants in this study.

Many mutations of the CaR cause loss of function by impairing normal expression of the receptor at the cell surface *(10,12,16)*. Therefore, we first tested cell surface expression of the mutant receptors by immunoblot. WT and mutant receptor cDNAs were transfected in HEK-293 cells and whole cell lysates immunoblotted with a monoclonal antibody, ADD, made against a peptide within the CaR ECD (*see* Fig. 1). As shown in Fig. 2A, under reducing conditions, ADD antibody detected two monomeric forms for the WT hCaR and for the mutants studied. Previous studies *(16,17)* demonstrated that the monomeric approx 150 kDa band represents hCaR forms expressed at the cell surface and modified with N-linked, complex carbohydrates; the approx 130 kDa band represents high-mannose-modified forms, trapped intracellularly and sensitive to Endo-H digestion. Lane 5 (Fig. 2A, TM1) represents the equivalent monomer forms for TM1 at approx 85 and 95 kDa migrating more rapidly because of the truncation of the remaining six transmembrane domains and C-tail. The appearance of the upper monomeric form of the receptor for all four mutants suggested that each is capable of reaching the cell surface. To confirm this, we biotinylated cell surface proteins in cells transfected with WT and mutant CaRs, used a specific monoclonal antibody raised against the purified CaR ECD to immunoprecipitate all CaR forms and then blotted with strepavidin to detect biotinylated, hence cell surface-expressed, CaR. Streptavidin identified only the upper, 150 kDa monomeric form of the WT CaR and missense mutants (Fig. 2B). The biotinylation experiment confirmed that all mutant receptors are capable of expression at the cell surface but the level of expression appeared to be reduced for D190A and E297K. The TM1 mutant (data not shown) routinely expresses at a level equal to or greater than WT *(8)*, whereas the cysteine-rich region deletion mutant is also capable of reaching the cell surface, albeit at lower levels when compared to the WT CaR *(15)*.

Reconstitution of Function

Since each of the five mutant forms of CaR was found to express at the cell surface, we tested their function by measuring the response of cells transfected with each receptor cDNA in a $[Ca^{2+}]_0$-stimulated PI hydrolysis assay. As shown in Fig. 3A, all three missense mutants showed severe functional impairment. A877-880E showed no response even up to 48 m*M* $[Ca^{2+}]_0$, while D190A and E297K showed a minimal response that was <10% of WT at the highest concentration tested. To test if mutants located in separate domains of the CaR could reconstitute function, we cotransfected D190A + A877-880E and E297K + A877-880E. In both cases, there was evidence of partial reconstitution of function with enhanced sensitivity (initial response seen at 8 m*M*) and increased maximal activity (D190A + A877-880E at approx 50% WT; E297K + A877-880E at approx 30% WT; Fig. 3A). We next tested the ability of the TM1 mutant, which, like A877-880E, has an intact ECD and expresses well at the cell surface to reconstitute function of the ECD missense mutants. Not surprisingly, the TM1 mutant, lacking most of the transmembrane domains and the entire C-tail, transfected alone fails to respond to $[Ca^{2+}]_0$ (Fig. 3B). Cotransfection of D190A + TM1 and of E297K + TM1, however, resulted in no reconstitution of function, but rather a slightly lower level of activity than seen with transfection of D190A or E297K alone (Fig. 3B). Given the failure of TM1 to reconstitute function when cotransfected with D190A or E297K, it was important to show that the TM1 mutant is capable of heterodimerizing with the ECD missense mutants, since heterodimerization is presumed necessary for reconstitution of function *(13)*. To test for heterodimerization, we used a coimmunoprecipitation assay with a polyclonal antibody, GGD, directed against a peptide epitope present in the C-tail of WT and ECD missense mutants but not in the truncated TM1 mutant (*see* Fig. 1). Transfection of TM1 alone followed by GGD immunoprecipitation and immunoblotting with the ADD monoclonal whose epitope is within the ECD shows only a nonspecific band (corresponding to IgG heavy chain band) running beneath the approx 85 kDa (intracellular form) of the TM1 mutant (Fig. 4, first lane). In contrast, when TM1 is cotransfected with WT CaR and subjected to GGD immunoprecipitation, the ADD blot reveals not only both monomeric forms of the WT receptor but also both the 95 kDa and 85 kDa bands of TM1 (the latter poorly resolved from the IgG heavy chain band referred to above; Fig. 4, second lane). Similarly, cotransfection of TM1 with either the D190A or E297K mutant leads to coprecipitation of TM1 although in amounts somewhat lower than for WT, consistent with the lower cell surface expression of the ECD missense mutants compared

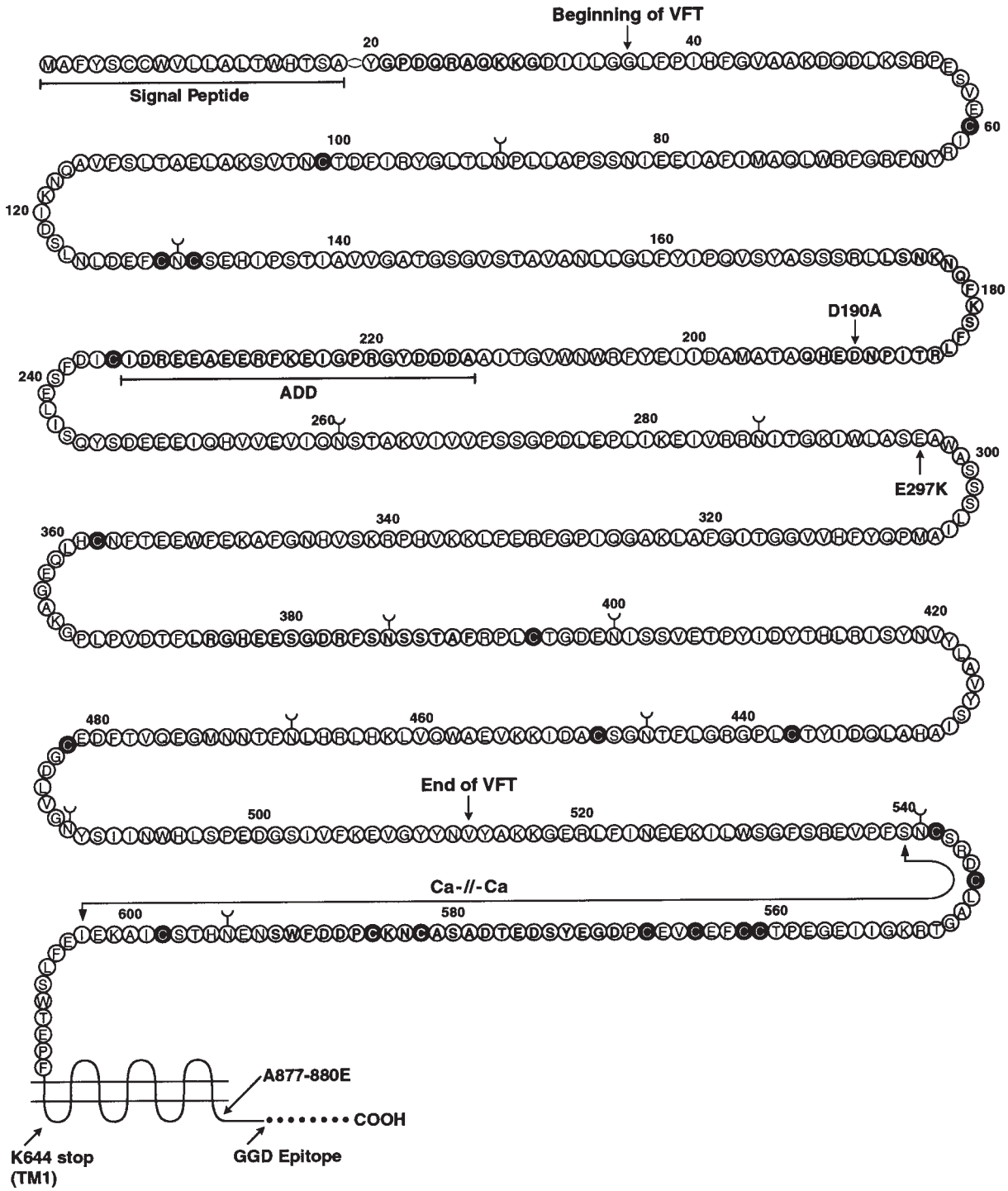

Fig.1. Schematic diagram showing structure of hCaR with amino acid sequence of ECD. The locations of signal peptide, N-linked glycosylation sites, and the epitopes for the monoclonal antibody ADD and polyclonal antibody GGD are indicated. All 19 cysteines are shown in black circles. The beginning and end of the putative VFT domain are indicated, as are the locations of the D190A, E297K, and A877-880E mutants. The arrowheads denote the cysteine-rich region of the ECD, which was deleted and substituted with five alanines in the Ca-//-Ca mutant. The position (Lysine 644) in the first intracellular loop used to create the TM1 mutant is also shown.

with WT. These results indicate that TM1 is capable of heterodimerizing with both WT and ECD missense mutants.

We next tested whether the cotransfection of the ECD inactivating mutant D190A with the deletion mutant Ca-//-Ca, which lacked the cysteine-rich region but still has the bilobed venus flytrap domain intact, would be able to recover function. As shown in Fig. 5, Ca-//-Ca by itself does not respond to calcium and was unable to recover

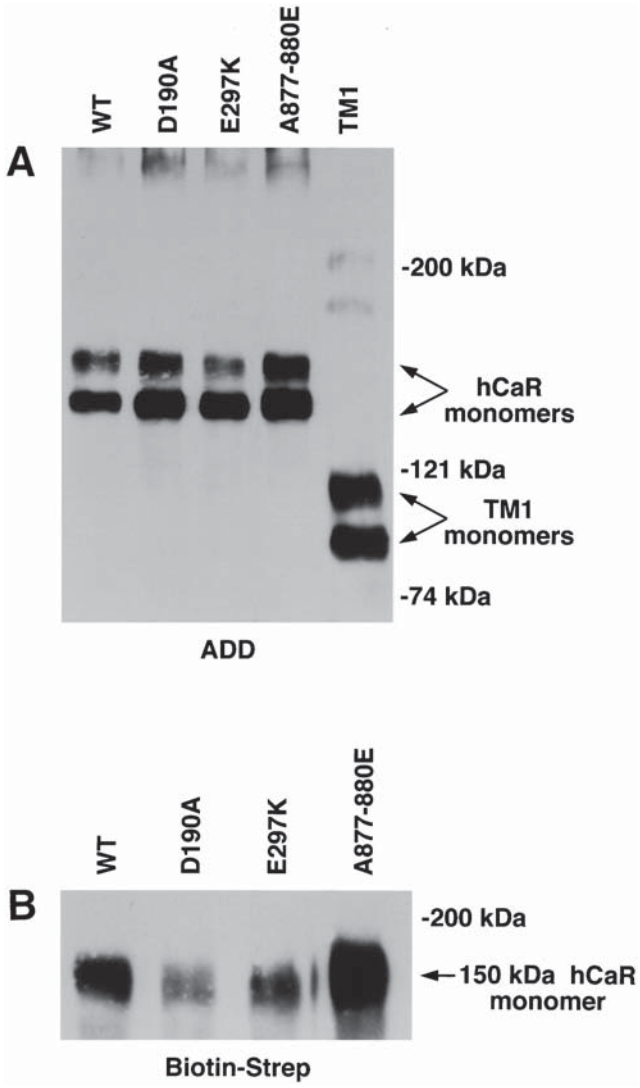

Fig. 2. Determination of cell surface expression of wild-type and mutant hCaRs. HEK-293 cells were transfected either with WT hCaR or with mutant forms of the CaR and receptor expression was studied by immunoblot **(A)** and cell surface protein biotinylation **(B)**. **(A)** Whole cell lysates were eluted with SDS-PAGE loading sample buffer containing β-mercaptoethanol, separated on 5% SDS-PAGE, and immunoblotting performed with anti-hCaR ADD monoclonal antibody. The positions of 200, 121, and 74 kDa molecular mass standards and of the bands representing hCaR and TM1 monomers are indicated on the right. **(B)** Cell surface proteins were labeled with Biotin-7-NHS as described in Methods. The cell lysates were immunoprecipitated with anti-hCaR 7F8 monoclonal antibody, and immunoprecipitates separated by SDS-PAGE. Biotinylated forms of WT and mutant receptors were detected with peroxidase-conjugated streptavidin.

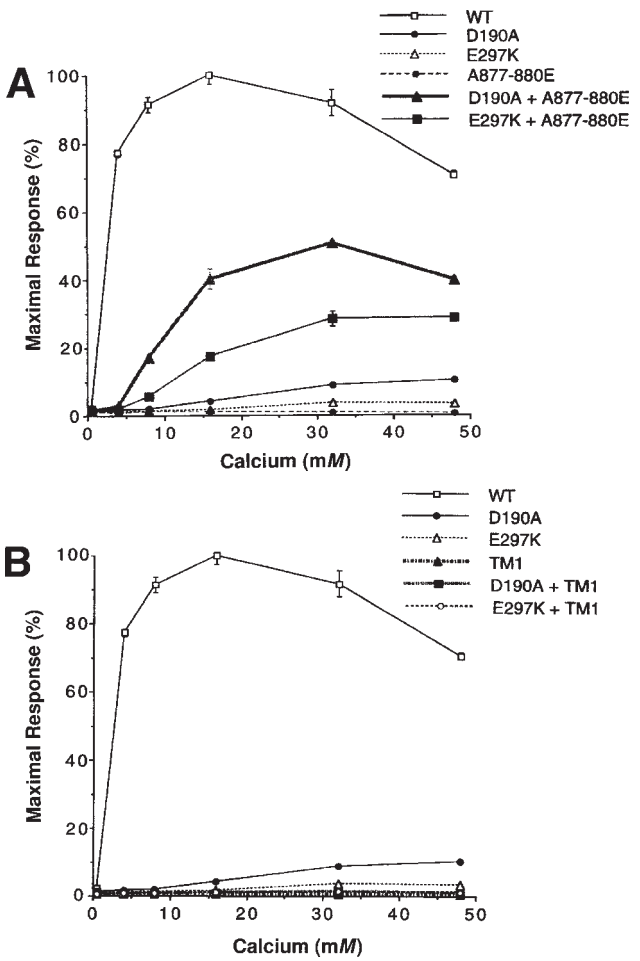

Fig. 3. Concentration-dependence for Ca^{2+} stimulation of phosphoinositide (PI) hydrolysis: evaluation of reconstitution of function. HEK-293 cells were transfected with WT and mutant hCaR cDNAs as described in Methods. **(A)** Ca^{2+} stimulation of PI hydrolysis for each inactivating mutant alone and for cotransfection of D190A + A877-880E and of E297K + A877-880E. **(B)** Ca^{2+} stimulation of PI hydrolysis for D190A, E297K, and TM1 alone and for D190A + TM1 and E297K + TM1. Data are the mean ± SEM of duplicate determinations from one of three to six experiments. Results (cpm of labeled total inositol phosphates generated) are expressed as a percent of the maximal response of the WT hCaR at 16 m*M* $[Ca^{2+}]_0$.

function when cotransfected with D190A (as shown in the inset of Fig. 5, Ca-//-Ca is expressed at the cell surface, albeit at lower levels when compared to the WT hCaR). Moreover, coexpression of this deletion mutant with the inactivating C-tail mutant A877-880E (which in turn has the cysteine-rich region intact) also did not lead to reconstitution of function (Fig. 5).

Discussion

In the present study, we tested the activity of mutants selected to probe the function of discrete domains, the ECD (namely, venus flytrap domain and cysteine -rich region) and 7TM/C-tail, of the CaR. The mutants were tested by themselves and in combination. The results provide new insights into the function of this receptor. Without a rigorously determined three-dimensional structure for any part of the CaR, any inferences about structure drawn from studies with site-directed mutants are necessarily speculative. Nonetheless, a model suggesting a bilobed, venus flytrap-like structure for the CaR ECD *(8)*, based on alignment of this portion of the ECD with the homologous mGluR and

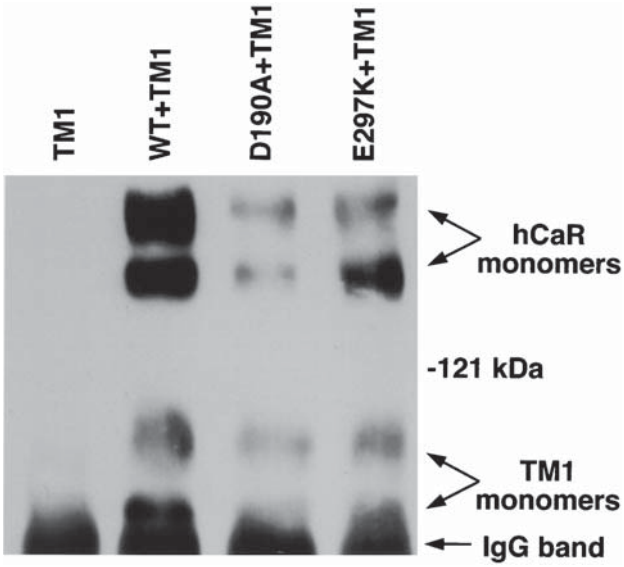

Fig. 4. Immunoprecipitation to detect heterodimerization of cotransfected WT and full-length mutant receptors with TM1 mutant receptor. HEK-293 cells were transfected with WT, D190A, or E297K receptor mutants along with TM1 as indicated in the figure. Cells were lysed and immunoprecipitation with anti-hCaR polyclonal antibody GGD was performed as described in Methods. Immunoreactive proteins were eluted with SDS-PAGE loading sample buffer containing β-mercaptoethanol and separated on 5% SDS-PAGE. Immunoblot was developed with anti-hCaR monoclonal antibody ADD. This blot is representative of several different transfections.

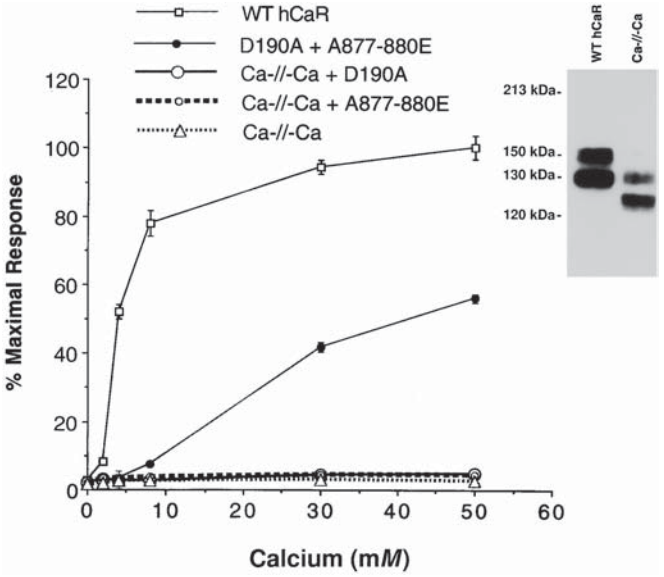

Fig. 5. Concentration-dependence for Ca^{2+} stimulation of phosphoinositide (PI) hydrolysis: evaluation of reconstitution of function. HEK-293 cells were transfected with WT and mutant hCaR cDNAs as described in Methods and Ca^{2+} stimulation of PI hydrolysis was performed for the cysteine-rich deletion mutant (Ca-//-Ca) alone and for cotransfection of Ca-//-Ca with D190A and with A877-880E. Results for cotransfection of D190A + A877-880E are also shown. Data are the mean ± SEM of duplicate determinations from one of three to six experiments. Results (cpm of labeled total inositol phosphates generated) are expressed as a percent of the maximal response of the WT hCaR at 50 m*M* $[Ca^{2+}]_0$. The inset shows an immunoblot performed with anti-hCaR ADD monoclonal antibody comparing the expression levels of WT hCaR and Ca-//-Ca. The upper band in both lanes corresponds to the form of the receptor expressed at the cell surface.

the bacterial PBP *(18)*, provides a useful basis for testing hypotheses concerning structure and function.

The two ECD missense mutants we studied both involve amino acids, D190 and E297, that are highly conserved not only in most family 3 GPCRs *(3,14)*, but also in bacterial PBPs such as the *Escherichia coli* leucine/isoleucine/valine binding protein (LIVBP) *(18)*. E297K is a naturally occurring loss of function mutation identified in FHH *(13)*. While many FHH mutations impair CaR folding and/or processing, thereby preventing cell surface expression *(16)*, the E297K mutant is expressed at the cell surface, albeit at lower levels than WT levels, so that loss of function cannot be explained by abnormal trafficking alone. Instead, it is likely that E297, whose equivalent residue is located at the end of a beta sheet in lobe 1 of *E. coli* LIVBP, serves a critical role in the normal activation mechanism of the CaR. Interestingly, three other missense mutations identified in FHH, G143E, R185Q, and Y218S, likewise involve residues conserved in the venus flytrap structure of LIVBP *(18)*.

We created the D190A mutant to test further this model of the CaR ECD structure. The residue equivalent to D190 is again conserved in most family 3 GPCRs and in LIVBP *(14,18)*. This residue is located in a strand that crosses from lobe 1 of the LIVBP flytrap to lobe 2, a hinge region known to be important in PBP function *(18)*. Like E297K, D190A showed some reduction in cell surface expression but a much greater overall loss of function, supporting a critical role in receptor activation. Of particular interest is the finding that the adjacent residue in the CaR, E191, is naturally mutated to lysine in a disease with opposite phenotype to FHH, namely, autosomal dominant hypocalcemia *(2)*. Gain of function mutations identified in the latter disease enhance sensitivity of the CaR to activation. Unlike D190, E191 is not conserved in other family 3 GPCRs or in LIVBP, suggesting a CaR-specific function. To determine the importance of the specific amino acid substituted for D190 and E191, in addition to D190A and E191K, we created and tested the reciprocal mutants, D190K and E191A. D190K did not cause gain of function but rather had the same loss of function phenotype as D190A; in contrast, E191A behaved like WT (O.M.H. and A.M.S., unpublished observations). This suggests an important functional difference between D190 and E191. Substitution of E191 with positively charged lysine rather than neutral alanine was required to cause increased receptor sensitivity, but the identical substitution for adjacent D190 was unable to enhance receptor activation.

It is tempting to speculate that residues such as D190, E191, and E297 are directly involved in Ca^{2+} binding, and that the changes in CaR activation seen upon mutation of these residues reflects such a role in Ca^{2+} binding. Lack of an assay to measure directly Ca^{2+} binding to the CaR, however, precludes such an inference. While studies with CaR/metabotropic glutamate receptor chimeras indicate that the ECD is the site of Ca^{2+} binding *(4,5)*, specific residues involved in this process have not been definitively identified. An alignment of the CaR with metabotropic glutamate receptors suggested the possibility that serines 147 and 170 in the rat CaR may be directly involved in Ca^{2+} binding, and mutation of these residues resulted in loss of Ca^{2+} activation providing supportive evidence *(5)*. Such mutagenesis studies, however, cannot prove a direct role in Ca^{2+} binding, since indirect effects on protein folding, for example, could account for loss of Ca^{2+} activation.

The A877-880E mutant created in the proximal C-tail, like the ECD mutants, lacked function despite adequate cell surface expression. Based on previous studies *(10)*, we suggest that the proximal C-tail is critical for G protein coupling, and that defective G protein coupling is the basis for loss of function of the A877-880E mutant. In the case of the TM1 mutant, lacking most of the 7TMs and entire C-tail domain, lack of G protein coupling and therefore function is predictable. It is, however, interesting that unlike CaR mutants truncated in the second or third intracellular loops, which are abnormally processed and fail to reach the cell surface *(10)*, the TM1 mutant shows excellent cell surface expression. The TM1 mutant, moreover, is capable of both homo- and heterodimerization, consistent with the importance of intermolecular disulfide bonding of cysteines in the ECD for CaR dimerization *(7,8)*. Thus, the TM1 mutant provides a useful tool for probing the role of the CaR ECD vs 7TM/C-tail in receptor function.

In this regard, the studies of Bai et al., *(13)* are of particular interest. These authors showed that coexpression of mutant CaRs with different ECD mutations failed to reconstitute function, but coexpression of an ECD mutant with a C-tail mutant, and to a lesser extent, a third intracellular loop mutant, did lead to reconstitution of function *(13)*. We were able to confirm these results in our coexpression of either the D190A or E297K ECD mutants with the C-tail mutant, A877-880E. Both combinations showed significant reconstitution of function, albeit below WT levels. This recovery of function is not explained by enhanced cell surface expression, but rather reflects functional interactions between the WT ECD of the A877-880E mutant and the WT 7TM/C-tail of either the D190A or E297K mutants. In contrast, coexpression of TM1 and either D190A or E297K led to no recovery of function, despite the ability of these mutant receptors to heterodimerize and reach the cell surface. In fact, coexpression reduced activity below that seen with D190A or E297K alone, presumably reflecting reduced expression of the respective homodimers caused by TM1 heterodimerization. The key question then is why does TM1, with a WT ECD that should be capable of communicating with the WT 7TM/C-tail of the D190A or E297K mutants, not lead to reconstituted function. Failure to see reconstitution with TM1 suggests that a single WT ECD and 7TM/C-tail within a heterodimer is insufficient for receptor activation. This could reflect a need for noncovalent interactions between each monomer 7TM/C-tail in addition to the ECD intermolecular disulfides in forming functional dimers.

No reconstitution of function was observed when the inactivating ECD mutant D190A was coexpressed with a CaR deletion mutant lacking only the cysteine-rich region located in the ECD. Also, coexpression of this deletion mutant with the A877-880E C-tail mutant did not lead to recovery of function. We were unable to use the coimmunoprecipitation assay to test directly the ability of the cysteine-rich region deletion mutant and either the ECD or C-tail mutants to heterodimerize, since all these mutants retain the GGD peptide epitope located in the C-tail. The cysteine-rich region deletion mutant, however, retains the cysteines (C129 and C131) we have previously shown to be critical for intermolecular disulfide-linked dimerization of the CaR *(8)*. We have, moreover, previously shown that the cysteine-rich region deletion mutant is capable of heterodimerizing when cotransfected with the TM1 mutant *(15)*, making it unlikely that failure to recover activity when cotransfected with the D190A or A877-880E mutants is due to inability of Ca-//-Ca to form heterodimers. Thus, it appears that both monomers must retain an intact cysteine-rich region in order for heterodimerization to allow reconstitution of function.

In conclusion, we have utilized mutants involving the ECD, 7TM, and C-tail domains of the CaR, to show that CaR activation involves functional interactions between these discrete domains and to define some of the structural requirements that are critical for this activation in the context of the dimeric receptor. Our data are consistent with, but certainly do not prove, a speculative model of receptor structure and function in which the receptor ECD, a bilobed, venus flytrap-like structure binds Ca^{2+} undergoing a conformational change (flytrap closure?) that leads to interaction with the 7TM domain and thereby G protein coupling. Further biochemical and structural studies are needed to test the validity of this model.

Materials and Methods

Site-Directed Mutagenesis

The hCaR cDNA construct subcloned in the pCR3.1 vector has been described *(10)*. Site-directed mutagenesis was performed using the QuickChange™ site-directed mutagenesis kit (Stratagene Inc., La Jolla, CA), according

to the manufacturer's instructions. In summary, a pair of complementary primers (sequence available from the authors upon request) with 30–40 bases was designed for each mutagenesis and the desired point mutation, D190A or E297K, was placed in the middle of the primers. For the mutant termed A877-880E, appropriate primers were designed to replace alanines in positions 877, 878, and 880 with glutamates. A truncation mutant containing the ECD and first transmembrane domain (termed TM1) was generated by introducing a stop codon in the first intracellular domain of the WT hCaR clone at amino acid position lysine 644. Parental hCaR inserted in pCR3.1 was amplified using Pfu Turbo DNA polymerase with these primers for 15 cycles in a DNA thermal cycler (Perkin-Elmer, Norwalk, CT). After digestion of the parental DNA with Dpn I for 1 h, the amplified DNA with the nucleotide substitution incorporated was transformed into *E. coli* (DH-5α strain). A deletion mutant lacking the cysteine-rich region located in the ECD of the CaR was constructed as described *(15)*. The mutations were confirmed by automated DNA sequencing using a Taq DyeDeoxy Terminator Cycle Sequencing kit and ABI prizm-377 DNA sequencer (Applied Biosystems, Foster City, CA).

Transient Transfection of WT and Mutant Receptors in HEK-293 Cells

Receptor cDNAS in pCR3.1 were prepared with a QIAGEN maxi Plasmid Maxi DNA preparation kit (QIAGEN Inc., Chatsworth, CA) and were introduced into HEK-293 cells by the Lipofectamine transfection method (Life Technologies Inc.). For transfection, a given amount of the plasmid DNA was diluted in Dulbecco's modified Eagle's medium (DMEM) (BioFluids Inc., Rockville, MD) and mixed with diluted Lipofectamine, and the mixture was incubated at room temperature for 30 min. The DNA–Lipofectamine complex was further diluted in serum-free DMEM and 12 μg of DNA was added to 80–90% confluent HEK-293 cells plated in 75 cm^2 flasks. When working with six-well plates, 2 μg of DNA was used for single plasmid transfection and for cotransfection experiments we added 1 μg of each of two different plasmids. After 5 h of incubation, an equal volume of DMEM containing 10% fetal bovine serum (FBS) (BioFluids Inc., Rockville, MD) was added and the media were replaced 24 h after transfection with complete DMEM containing 10% FBS. Membrane protein extraction for immunoblotting, whole cell enzyme-linked immunoassay, or phosphoinositide (PI) hydrolysis assay were performed 48 h after transfection.

Biotinylation of Cell Surface CaR

Forty-eight hours after transfection, cell surface proteins of the intact HEK-293 cells were labeled with membrane-impermeant Biotin-7-NHS using the cellular labeling kit (Boehringer Mannheim, Indianapolis, IN). Briefly, adherent cells were washed once with ice-cold phosphate-buffered saline (PBS), treated with 50 μg/mLof Biotin-7-NHS in biotinylation buffer (50 m*M* sodium borate, 150 m*M* NaCl) for 15 min at room temperature to biotinylate cell surface proteins. The reaction was stopped by adding 50 m*M* NH_4Cl for 15 min on ice. The cells were washed twice with ice-cold PBS and solubilized with 1 mL buffer-B per well containing 1% Triton-X100, 20 m*M* Tris-HCl (pH 6.8), 150 m*M* NaCl, 10 m*M* EDTA, 1 m*M* EGTA with freshly added protease inhibitor cocktail. To prevent nonspecific disulfide bond formation during protein extraction, the intact cells were incubated and washed in PBS containing 50 m*M* iodoacetamide, and 10 m*M* iodoacetamide was included in the lysis buffer.

Immunoprecipitation of CaR

Three hundred microliters (approx 600 μg total protein) of the whole cell lysate prepared by scraping cells from six-well plates in buffer-B (as described above) was further diluted with 300 μL of buffer-B and incubated with either 5 μL of 7F8 mouse monoclonal hCaR-specific antibody (made against the purified hCaR ECD; 1 mg/mL stock) or 7 μL of affinity-purified rabbit polyclonal hCaR-specific antibody GGD (made against a synthetic peptide corresponding to amino acids 1037 to 1050 of the hCaR protein; 1 mg/mL stock) for 90 min at 4°C. Subsequently, 25 μL of Protein A/G (for 7F8) or Protein A (for GGD) agarose (Santa Cruz Biotech., Santa Cruz, CA) was added and further incubated for an additional 90 min at 4°C. The Protein A/G or A agarose was washed three times with buffer-B containing 0.5% SDS, and the immunoreactive proteins were eluted in 120 μL of 1X sample buffer containing 300 m*M* β-mercaptoethanol at room temperature for 5 min. Fifty microliters of sample were loaded per lane and immunoblotting was performed as described in the next section.

Immunoblotting Analysis with Detergent-Solubilized Whole Cell Extracts

Confluent cells in 75 cm^2 flasks or six-well plates were rinsed with PBS and scraped on ice in buffer-B containing 20 m*M* Tris-HCl (pH 6.8), 150 m*M* NaCl, 10 m*M* EDTA, 1 m*M* EGTA, 1% Triton X-100 with freshly added protease inhibitors cocktail (Complete, Boehringer Mannheim, Indianapolis, IN). The protein content of each sample was determined by the modified Bradford method (Bio-Rad, Hercules, CA) and 40–60 μg of protein per lane was separated on 5% SDS-PAGE. The proteins on the gel were electrotransferred to nitrocellulose membrane and incubated for 90 min with protein A-purified mouse monoclonal anti-hCaR antibody ADD (raised against a synthetic peptide corresponding to residues 214–235 of hCaR protein) *(19)* at a dilution of 1:10000. After washing three times for 15 min with Tris-buffered saline with Tween (TBST, containing 0.05 *M* Tris, pH 8.0, 0.05 *M* NaCl with 0.1% Tween 20), the membrane was incubated for 90 min with a second-

ary goat anti-mouse antibody conjugated to horseradish peroxidase (Kierkegaard and Perry Laboratories Inc., Gaithersburg, MD) at a dilution of 1:5000. After washing three times for 15 min with TBST and once for 15 min with Tris-buffered saline, the hCaR protein was detected with an Enhanced Chemiluminescence system (Amersham Corp, Arlington Heights, IL).

Phosphoinositide (PI) Hydrolysis Assay

PI hydrolysis assay has been described *(10,20)* Briefly, 24 h after transfection, transfected cells from a confluent 75 cm^2 flask were replated in a 12-well plate in medium containing 3.0 μCi/mLof ^{3}H-myoinositol (New England Nuclear, Beverly, MA) in complete DMEM for another 24 h, followed by 1 h incubation with 1 X PI buffer (120 m*M* NaCl, 5 m*M* KCl, 5.6 m*M* glucose, 0.4 m*M* $MgCl_2$, 20 m*M* LiCl in 25 m*M* PIPES buffer, pH 7.2). After removal of PI buffer, cells were incubated for an additional 1 h with different concentrations of $[Ca^{2+}]_0$ in PI buffer. The reactions were terminated by the addition of 1 mL of acid-methanol (167 μL of HCl in 120 mL of methanol). Total inositolphosphates were purified by chromatography on Dowex 1-X8 columns.

Acknowledgments

We are grateful to Regina Collins for superb assistance with cell culture and to Paul Goldsmith for assistance with antibodies and ELISA.

References

1. Brown, E. M., Gamba, G., Riccardi, D., Lombardi, M., Butters, R., Kifor, O., et al. (1993). *Nature* **366,** 575–580.
2. Brown, E. M. (1999). *Am. J. Med.* **106,** 238–253.
3. Bockaert, J. and Pin, J. P. (1999). *EMBO J.* **18,** 1723–1729.
4. Hammerland, L. G., Krapcho, K. J., Garrett, J. E., Alasti, N., Hung, B. C. P., Simin, R. T., et al. (1999). *Mol. Pharmacol.* **77,** 642–648.
5. Bräuner-Osborne, H., Jensen, A.A., Sheppard, P. O., O'Hara, P., and Krogsgaard-Larsen, P. (1999). *J. Biol. Chem.* **274,** 18,382–18,386.
6. von Heijne, G. (1986). *Nucleic Acids Res.* **14,** 4683–4690.
7. Goldsmith, P. K., Fan, G. F., Ray, K., Shiloach, J., McPhie, P., Rogers, K. V., and Spiegel, A. M. (1999). *J. Biol.Chem.* **274,** 11,303–11,309.
8. Ray, K., Hauschild, B. C., Steinbach, P. J., Goldsmith, P. K., Hauache, O., and Spiegel, A. M. (1999). *J. Biol. Chem.* **274,** 27,642–27,650.
9. Bai, M., Janicic, N., Trivedi, S., Quinn, S. J., Cole, D. E. C., Brown, E. M., and Hendy, G. N. (1997). *J. Clin. Invest.* **99,** 1917–1925.
10. Ray, K., Fan, G. F., Goldsmith, P. K., and Spiegel, A. M. (1997). *J. Biol. Chem.* **272,** 31,355–31,361.
11. Bai, M., Trivedi, S., and Brown, E. M. (1998). *J. Biol. Chem.* **273,** 23,605–23,610.
12. Fan, G. F., Ray, K., Zhao, X. M., Goldsmith, P. K., and Spiegel, A. M. (1998). *FEBS Lett.* **436,** 353–356.
13. Bai, M., Trivedi, S., Kifor, O., Quinn, S. J., and Brown, E. M. (1999). *Proc. Natl. Acad. Sci. USA* **96,** 2834–2839.
14. Hoon, M. A., Adler, E., Lindemeier, J., Battey, J. F., Ryba, N. J. P., and Zuker, C. S. (1999). *Cell* **96,** 541–551.
15. Hu, J., Hauache, O., and Spiegel, A. M. (2000). *J. Biol. Chem.* **275,** 16,382–16,389.
16. Bai, M., Quinn, S., Trivedi, S., Kifor, O., Pearce, S. H. S., Pollak, M. R., et al. (1996). *J. Biol. Chem.* **271,** 19,537–19,545.
17. Ray, K., Clapp, P., Goldsmith, P. K., and Spiegel, A. M. (1998). *J. Biol. Chem.* **273,** 34,558–34,567.
18. O'Hara, P. J., Sheppard, P. O., Thogersen, H., Venezia, D., Haldeman, B. A., McGrane, V., et al (1993). *Neuron.* **11,** 41–52.
19. Goldsmith, P. K., Fan, G., Miller, J. L., Rogers, K. V., and Spiegel, A. M. (1997). *J. Bone. Miner. Res.* **12,** 1780–1788.
20. Fan, G., Goldsmith, P. K., Collins, R., Dunn, C. K., Krapcho, K. J., Rogers, K. V., and Spiegel, A. M. (1997). *Endocrinol.* **138,** 1916–1922.